Dynamic Response of Some Ion-Selective Electrodes

The dynamic responses of five electrodes were measured by pulse testing. The electrodes were three pH electrodes; a calcium-ion electrode, and a chloride-ion electrode. Measurements were made at temperatures from 1° to 50°C. The responses of their electrodes were analyzed to give the transfer function containing first- and second-order time constants and a dead time.

PATRICK L. MARKOVIC and JAMES O. OSBURN

Department of Chemical Engineering
University of Iowa
Iowa City, Iowa 52240

SCOPE

When the concentration of a solution changes with time, the change in the electrical signal produced by an ion-selective electrode immersed in the solution lags behind the concentration change. The relationship between the change in electrode potential and the concentration change is the dynamic response, usually described by a Bode or Nyquist diagram, or by a transfer function. The dynamic response helps determine the kind of control that can be achieved by automatic control systems.

This article reports the results of measurements of the dynamic response of two hydrogen-ion electrodes, a calcium-ion electrode, and a chloride-ion electrode. The measurements, made by pulse testing, covered a range of temperature, and a computer was used to perform the frequency analysis of the data.

CONCLUSIONS AND SIGNIFICANCE

Each *p*H electrode responded as a first-order system; the responses of the calcium and chloride electrodes were second order. Only the calcium electrode response included a dead time. Time constants of up to 10 seconds were observed at low temperature. With a time constant of this magnitude, the response of the electrode would be an important consideration in the control system for concentration control in which the concentration was changing rapidly.

The transfer function is shown to correspond to the physical structure of the electrode with time lags due to diffusional transfer of ions. The diffusional nature of the process is deduced from the variation of the time constant with temperature.

The hydrogen ion or *p*H electrode is a widely used analytical device. Recently a number of ion-selective electrodes have been developed for the analysis of other ions in solution.

When these electrodes are used for the analysis of individual samples, the response time is not very important. The analyst can leave the electrode in the sample long enough to ensure equilibrium. However, when they are used as sensing devices in control systems, the response time of the electrode introduces a time delay into the control loop and might even lead to instability in some cases.

Some studies have been made (Disteche, 1954; Geerlings, 1957; Giusti, 1960; Hougen, 1964; Ross, 1969; Licht, 1969) on the dynamic response of *p*H electrodes. There has been much variability in the results reported.

THEORY

Ross (1969) points out that when an electrode is placed in a sample solution, there is a momentary flux of ions across the membrane in the direction of the solution containing the lower activity of the mobile ion. These ions carry a charge so that an electrical potential is established which opposes further ion migration. Thus, at steady state conditions, an equilibrium is established in which the potential across the membrane is exactly that required to prevent further net movement of ions.

The membrane potential is measured by making electrical contact with the inner solution by an internal reference electrode and at the same time contacting the sample solution with a reference electrode via a salt bridge. A high impedance voltmeter indicates the potential, as shown in Figure 1.

The dynamic characteristics of electrodes relate to the flux of ions across the membrane so that diffusion of the ionic species being measured determines the speed and mode of electrode response.

Geerlings (1957), Harriott (1964), and Murrill (1967) point out that in the case of *p*H glass membrane electrodes, it is the diffusion through the boundary layer around the electrode that is rate-controlling. Disteche and Dubisson (1954) measured a first-order response time for the glass membrane of about 30 ms, independent of membrane thickness.

Thus, according to Harriott (1964), the major factors affecting the electrode response are the thickness of the boundary layer around the electrode, the concentrations

Correspondence concerning this paper should be addressed to J. O. Osburn. P. L. Markovic is with E. I. duPont de Nemours and Co., Inc., Clinton, Iowa.

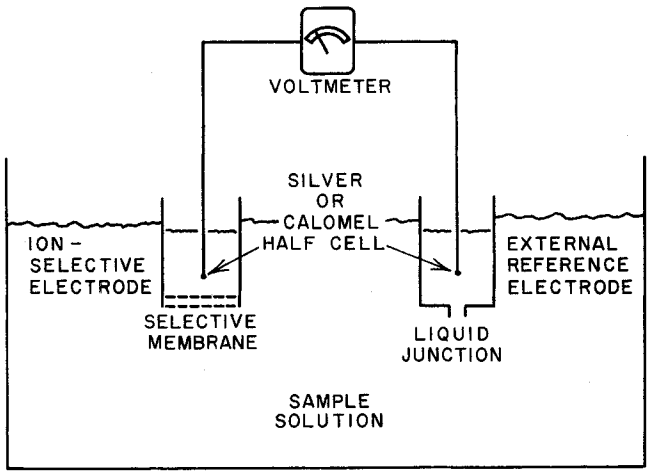

Fig. 1. Schematic diagram of the apparatus used in ion-selective electrode measurement (Ross, 1969).

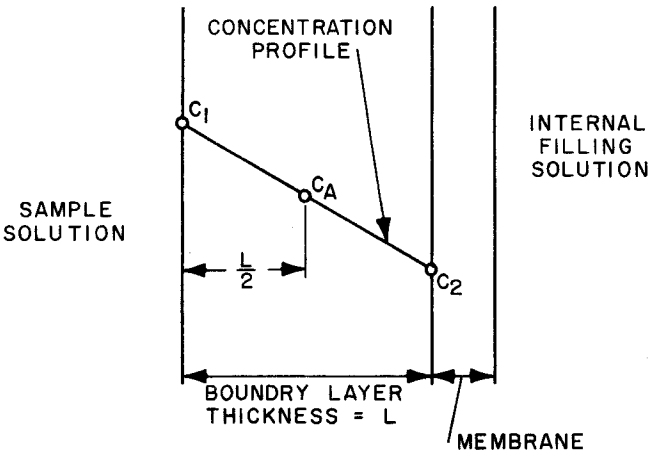

Fig. 2. Diffusion model for mass transfer in ion-selective electrode.

and diffusivities of the various ions, and the holdup of ions of the membrane. Considering the ion capacity of the membrane to be negligible, the effective time constant may be obtained from the capacity of the liquid layer around the electrode and the resistance to diffusion.

Consider the model shown in Figure 2 with no flux from the boundary layer to the membrane. The following expression relates the variation of c_A to time:

$$A \cdot L \cdot \frac{dc_A}{dt} = \frac{-D \cdot A \cdot (c_A - c_1)}{L/2} \tag{1}$$

which simplifies to

$$\frac{dc_A}{dt} = \frac{-2 \cdot D \cdot (c_A - c_1)}{L^2} \tag{2}$$

Assuming c_A and its derivatives are initially zero, the LaPlace transform of Equation (2) is

$$s \cdot c_A(s) = \frac{-2 \cdot D}{L^2} (c_A(s) - c_1(s)) \tag{3}$$

which, upon rearrangement and simplification, becomes

$$\frac{c_A(s)}{c_1(s)} = \frac{1}{1 + (L^2/2 \cdot D)\, s} = \frac{1}{1 + \tau s} \tag{4}$$

where $\tau = L^2/2 \cdot D$. This is a first-order transfer function with a time constant τ, which agrees with the results of Geerlings (1957) and Harriott (1964).

The preceding analysis assumes a linear concentration profile through the boundary layer, which is a characteristic only of a steady state. A more reasonable model would be one derived from the unsteady state equation of Fick (1855):

$$\frac{\partial c}{\partial t} = D \frac{\partial^2 c}{\partial x^2} \tag{5}$$

If point c_2 in Figure 2 is taken to be at the center of a plane slab of thickness $2L$, with zero concentration c equal to zero at zero time in the region $-L < x < L$, and the concentrations equal to c_1 at the surfaces $x = \pm L$ with time t greater than zero, then the solution to Equation (5) becomes (Crank, 1970)

$$c = c_1 - \frac{4c_1}{\pi} \sum_{n=0}^{\infty} \frac{(-1)^n}{2n+1} \exp\left(\frac{-D(2n+1)^2\pi^2 t}{4L^2}\right) \cos\frac{(2n+1)\,\pi x}{2L} \tag{6}$$

The concentration c_2 at location $x = 0$ may be found by taking the first term of the infinite series as a first-order approximation. Equation (6) becomes

$$c_2 = c_1 - \frac{4c_1}{\pi} \exp\left(\frac{-D\pi^2 t}{4L^2}\right) \tag{7}$$

Equation (7) is differentiated to get

$$\frac{dc_2}{dt} = \left[-\frac{4c_1}{\pi} \exp\left(\frac{-D\pi^2 t}{4L^2}\right)\right]\left(\frac{-D\pi^2}{4L^2}\right) \tag{8}$$

Substituting Equation (7) into Equation (8) gives

$$\frac{dc_2}{dt} = (c_2 - c_1)\left(\frac{-D\pi^2}{4L^2}\right) \tag{9}$$

The LaPlace transform of Equation (9) is

$$sc_2(s) = -\frac{D\pi^2}{4L^2}(c_2(s) - c_1(s)) \tag{10}$$

Upon rearrangement and simplification, Equation (10) becomes

$$c_2(s)\left(s + \frac{D\pi^2}{4L^2}\right) = c_1(s)\,\frac{D\pi^2}{4L^2} \tag{11}$$

$$\frac{c_2(s)}{c_1(s)} = \frac{1}{1 + \frac{4L^2}{D\pi^2} s} = \frac{1}{1 + \tau s} \tag{12}$$

where $\tau = 4L^2/D\pi^2$. This is equivalent to the result obtained by Jost (1952). In either case, steady or unsteady state, the time constant is inversely proportional to the diffusion coefficient.

Murrill (1967) and Harriott (1964) considered a second time constant in the response of a pH electrode, one associated with the holdup and flow through the electrode cell. This time constant depends on V/F where V is the cell volume and F is the flow rate through the cell.

Harriott points out that in distributed systems or systems with many time constants in series, the initial response to a step change is sometimes imperceptible; while these systems have no true time delay, the response can be approximated by using an effective time delay plus one or more time constants.

Thus, the overall transfer function used by us corre-

sponds to two coupled first-order stages with an effective time delay, as follows:

$$G(s) = \frac{e^{-\tau_D s}}{(1 + \tau_1 s)(1 + \tau_2 s)} \tag{13}$$

The frequency response for this is

$$\text{Magnitude ratio, M.R.} = \frac{1}{\sqrt{(1 + (\tau_1\omega)^2)(1 + (\tau_2\omega)^2)}} \tag{14}$$

$$\text{phase angle, } \phi = \arctan(-\tau_1\omega) + \arctan(-\tau_2\omega) - \tau_D\omega \tag{15}$$

The apparent activation energy for diffusion, according to Jost (1952), can be calculated as

$$\Delta H^* = -R \cdot d(\text{Ln } D)/d(1/T) \tag{16}$$

If this apparent activation energy is constant over the temperature range being considered, then a plot of Ln D versus $1/T$ would be linear with the slope equal to $-\Delta H^*/R$. Thus, Equation (16) can be written as

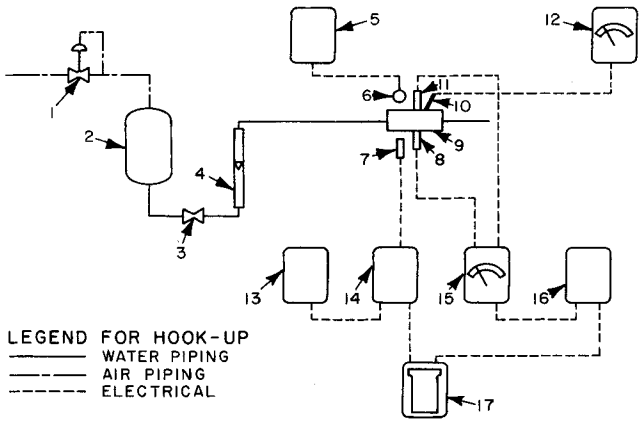

Fig. 3. Schematic diagram of apparatus: 1. Supply air pressure regulator; 2. Water supply tank; 3. Needle valve; 4. Rotameter; 5. Power supply for light source; 6. Light source; 7. Photocell; 8. Reference electrode; 9. Measuring cell; 10. Thermistor; 11. Ion-selective electrode; 12. Thermistor indicator; 13. Power supply for bridge circuit; 14. Bridge circuit; 15. pH meter; 16. Low band-pass filter; 17. Dual channel strip chart recorder.

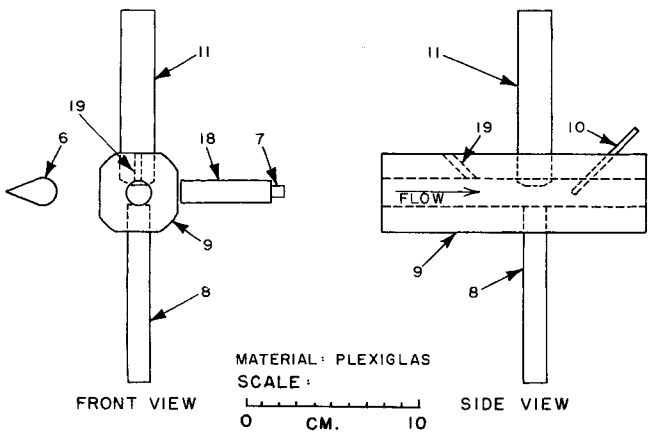

Fig. 4. Detailed schematic of test cell: 6. Light source; 7. Photocell; 8. Reference Electrode; 9. Measuring cell; 10. Thermistor; 11. Ion-selective electrode; 18. Photocell aiming tube; 19. Sample injection port.

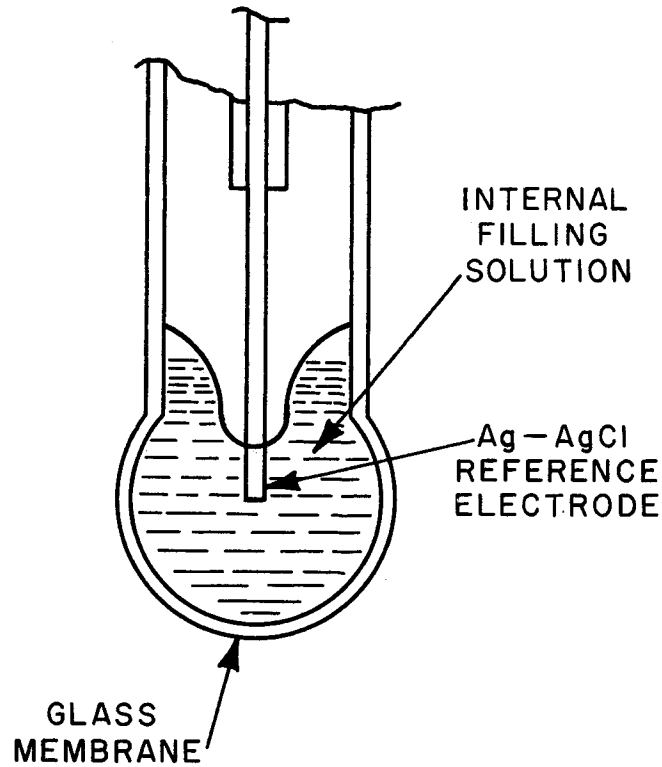

Fig. 5. Construction of conventional glass pH electrode (Light, 1969).

$$\text{Ln } D = m \cdot (1/T) + a_1 \tag{17}$$

where m is the slope and a_1 is the value of Ln D at an infinite temperature. To relate τ to temperature, substitute $D = 4L^2/\tau\,\pi^2$, as defined in Equation (12), into Equation (17), rearrange and simplify as follows:

$$\text{Ln } (4L^2/\tau\,\pi^2) = m \cdot (1/T) + a_1 \tag{18}$$

This reduces to

$$\text{Ln } \tau = -m(1/T) + a_2 \tag{19}$$

Equation (19) indicates that the plot of Ln τ versus $1/T$ is linear with a slope of $\Delta H^*/R$.

EXPERIMENT

The pulse-testing method described by Hougen (1964) was selected for this study because with it a broad frequency range can be covered with each experiment. The measurements needed are the system input pulse and the system output pulse. These two pulses are then compared using a digital computer program originally developed by Hays, Clements, and Schnelle (1964) to calculate the Bode diagram for the data.

The equipment is shown schematically in Figure 3. Water, at a preadjusted temperature, was forced out of the supply tank (#2) by air pressure. The water then flowed at a measured rate through the test cell (#9). Figure 4 shows this cell in detail. A solution of the ion species being tested was made opaque by the addition of ink. A 0.2 ml aliquot was injected through the sample injection port (#19) using a hypodermic syringe. The light source (#6) and photocell (#7) system measured the system input pulse by measuring the optical density.

The output pulse was the response of the ion-selective electrode (#11). The construction of the two types used is shown in Figures 5 and 6. The ion-selective electrode output was measured by the pH meter (#15), using the reference electrode to complete the circuit. High frequency noise in the recorder output from the pH meter was reduced by the low band-pass filter (#16). This signal was then amplified

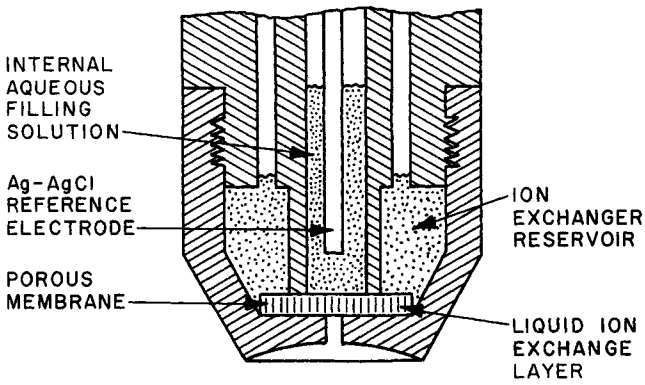

Fig. 6. Construction of liquid ion-exchange electrode (Orion Research, Inc).

and recorded by the strip chart recorder (#17). The resistance change of the photocell (#7) was measured by the Wheatstone bridge (#14) whose output was also amplified and recorded by the strip chart recorder.

Examples of strip chart recordings from three different experimental runs are shown in Figure 7. The tic marks along the bottom of the strip charts are one-second timing marks.

At the beginning of each series of experimental runs, the light system was calibrated using the opaque solution. This gave the relation between the optical density of the solution and the ionic activity. Errors due to changes in alignment of the light source and photocell system or aging of the light source or photocell were avoided by frequent checking of the calibration.

A number of points sufficient to describe the recorded input and output pulse curves were then read from the strip charts, as indicated by the marks on the charts shown in Figure 7. These points constituted the input to the computer program used to analyze the data.

CALCULATIONS

The computer program first converted the data into ionic activity, using the calibrations which had been made. Then, an order-of-magnitude estimate of the data errors was made. According to Hays (1964), when either the input or output normalized frequency content approaches the order of magnitude of the experimental error, the reliability of the calculated values of magnitude ratio and phase angle are unreliable.

The pulse reduction computer program next calculated the Bode diagram. From the calculated magnitude ratios, over the reliable frequency range, the two time constants from a coupled first-order transfer function were fitted. Equation (14) was used after suitable modification to take into account the instrumentation time constants.

The instrumentation time constants were measured by replacing the ion-selective electrode by a reference voltage source, which was used as input to the *p*H meter. The same signal was also used as input to the other channel of the recorder. A pulse in this reference voltage produced pulses in the recorded output. These were then analyzed using a computer program similar to the one used for the electrode data, with results as listed in Table 1.

The low band-pass filter was also tested for its frequency response by a sinusoidal method. It was found to have a first-order response, and its time constant agreed with the one obtained by the pulse testing method.

The photocell had a first-order response. However, its time constant was much smaller than the others, and so was neglected.

The instrument responses were used to modify Equation (14) and the two electrode time constants were obtained by fitting this equation to calculated magnitude ratios:

$$\text{M.R.} = [(1 + (\tau_1\omega)^2)(1 + \tau_2\omega)^2)(1 + (0.177\omega)^2)(1 + (0.076\omega)^2)(1 + (0.022\omega)^2)]^{-1/2} \quad (20)$$

The grid search routine of Mischke (1968) was used to select the numerical values of τ_1 and τ_2 that minimized the sum-of-squares deviations between the magnitude ratio values calculated by Equation (22) and those calculated from the data by the pulse analysis program. The magnitude ratio and phase angle values were calculated by the pulse analysis program at evenly spaced values of $\log\omega$. The same values of $\log\omega$ were used in determining the values of τ_1 and τ_2 in Equation (22).

The calculated phase angles were used to find the effective time delay. This was done by a one-dimensional optimization procedure, using this equation which includes the instrumentation response:

$$\phi = \omega\tau_D - \arctan(-\omega\tau_1) - \arctan(-\omega\tau_2) - \arctan(-0.177\omega) - \arctan(-0.076\omega) - \arctan(-0.022\omega) \quad (21)$$

The same values of ω were used to determine τ_D as were used to determine τ_1 and τ_2.

TABLE 1. INSTRUMENTATION TIME CONSTANTS

*p*H Meter:	
Larger time constant	0.177 s
Smaller time constant	0.076 s
Effective time delay	0.0004 s
Low Band-Pass Filter:	
First order	0.022 s
Photocell:	
First order	0.0024 s

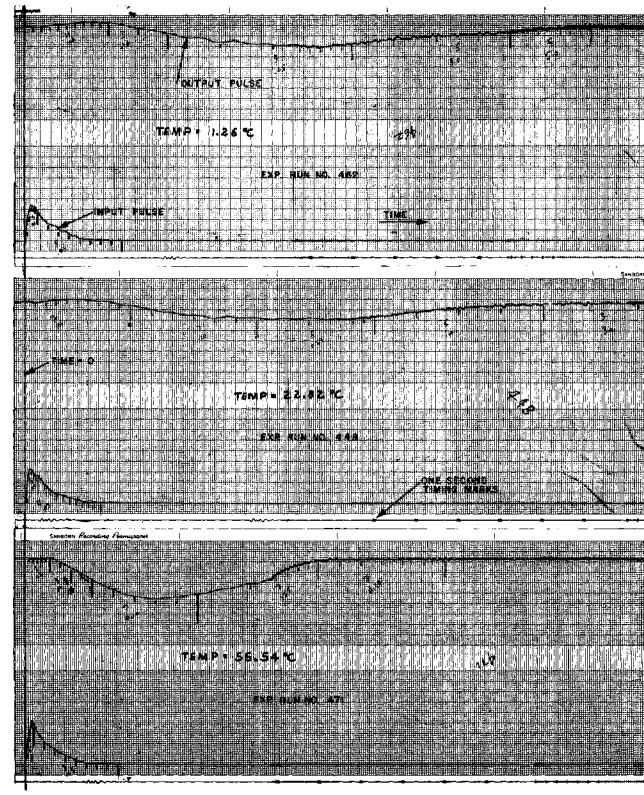

Fig. 7. Three typical recorder charts.

TABLE 2. TIME CONSTANTS FOR ION SELECTIVE ELECTRODES

$$\ln \tau = -A' + B/T$$

	A'	B	Correlation coefficient	at T, °K = 273	= 300	= 325	No. of measurements, N
Corning *p*H 476022	10.67	3509	0.90	8.87	2.79	1.14	100
Corning *p*H 476051	6.70	2265	0.87	4.94	2.34	1.31	45
Thomas *p*H 4855-B15	1.82	1125	0.73	9.98	6.89	5.22	50
Orion calcium 92-20							
First	11.70	3374	0.78	1.93	0.64	0.27	105
Second	13.75	3612	0.81	0.60	0.18	0.072	
Delay	25.06	6732	0.75	0.64	0.051	0.007	
Orion chloride 92-17							
First	13.07	4007	0.91	2.63	0.70	0.25	65
Second	21.31	5787	0.72	0.89	0.13	0.030	

RESULTS AND DISCUSSION

A total of 371 sets of measurements were made on the five electrodes. The calculation of time constants from pulse data results in an amplification of experimental errors, so there was considerable scatter in the data. This is illustrated by Figure 8 on which are plotted all the data points for one of the *p*H electrodes. To correlate the data, a linear least squares fit, to the Equation (22) was made:

$$\ln \tau = -A' + B/T \qquad (22)$$

In Table 2 are listed values of A' and B, the correlation coefficients, and the smoothed values of the time constants at three temperatures. The smoothed time constants are plotted in Figure 10 from which the large variation with temperature can be observed.

HYDROGEN-ION ELECTRODES

The *p*H electrodes responded as first-order systems. This response is in accord with the principles stated by Harriott (1964), who states that with measuring cells in which the holdup is low, the time constant associated with mixing in the cells tends to vanish. The measuring cell used in this study was a flow tube with very low holdup, so a first-order response would be expected.

Giusti (1960) reports time constants of from 0.25 to 8.5 seconds for *p*H electrodes. Although he does not give the temperatures at which measurements were made, it can be assumed that they were made at ambient temperature. Thus, they would fall in the range of our measurements at 300°K, which were from 2.8 to 6.9.

LIQUID MEMBRANE ION-SELECTIVE ELECTRODE

For the calcium and chloride ion-selective electrodes, values for both a first and a second time constant were significant. Values for an effective time delay constant were found for the calcium electrode, but for the chloride

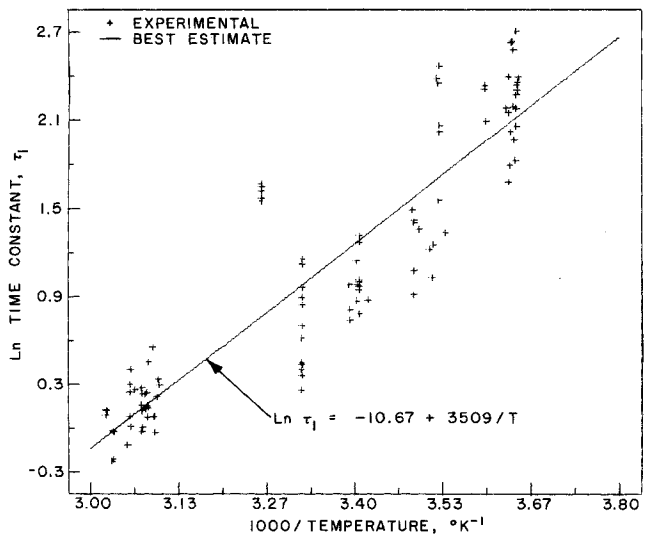

Fig. 8. Natural logarithm of first-order time constant versus the reciprocal of the absolute temperature for Corning *p*H electrode, Catalog No. 476022.

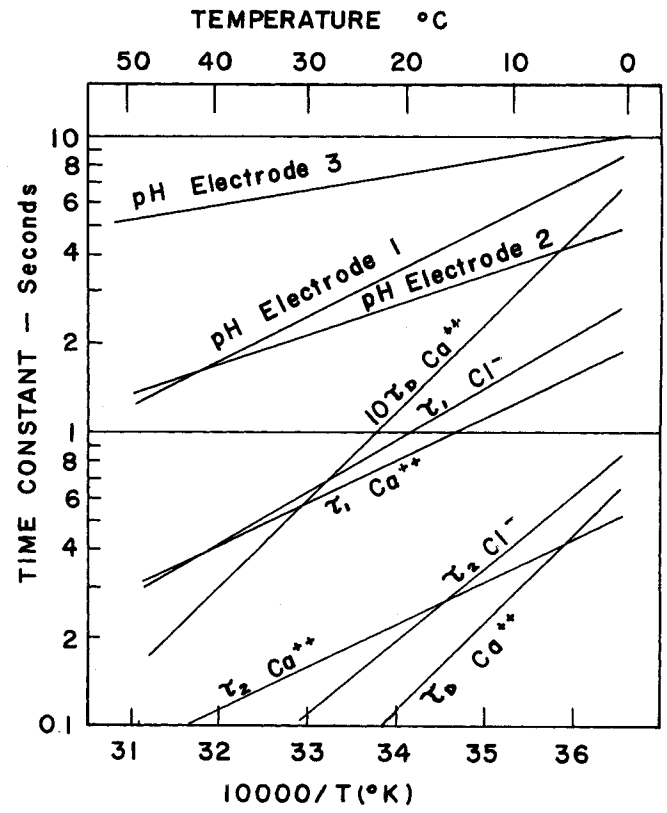

Fig. 9. Time constants of the electrodes plotted aginst 10,000/T.

Table 3. Activation Energy for Diffusion in Ion-Selective Electrodes

Electrode	Activation energy, Kjoule/mole
Corning *p*H 476022	29.3
Corning *p*H 476051	18.8
Thomas *p*H 4855-B15	9.2
Orion calcium 92-20	
First	28.0
Second	30.1
Orion chloride 92-17	
First	33.5
Second	48.1

electrode the time delay was essentially zero.

The variation of the effective time delay constant with temperature is shown in Figure 9 for the calcium electrode. The time delay shows the same pattern as the first and second time constants, which, as Harriott (1964) indicates, would be the case. As the overall system response slows down at lower temperatures, the length of time before a perceptible change in initial response to a step change would become longer. Thus, larger effective time delays would be required to model the system accurately.

The response of the liquid membrane electrodes is that of two consecutive first-order processes. The time constants for one process are roughly three times that of the other. The time constants for the two electrodes are very similar, except that there is a pure time delay associated with the calcium electrode.

For all the electrodes, the time constants vary significantly with temperature. This can be explained in terms of the diffusion of ions.

A time constant is the result of a combination of capacitance and resistance. The capacitance is a volume where ions or electrons can accumulate. The resistance may be a flow restriction or a film through which diffusion takes place. The resistance of a restriction does not vary with temperature, while diffusion does.

The two electrodes were identical in physical dimensions since the same electrode body was used by both. The change in ion selectivity was obtained by changing the membrane, the liquid ion exchanger, and the internal filling solution. The capacitance effect is, therefore, the same for both electrodes and should be independent of temperature.

The effect of temperature is evidently due to the effect of temperature on the diffusion of ions through the liquid film surrounding the electrode and through the filling solution. Diffusion varies with temperature as shown by Equation (17) and the activation energies are proportional to the slope of the line.

The values of activation energy of diffusion calculated from the time constant data are shown in Table 3. Jost (1952) gives values of 6.3 to 22.2 Kjoule/mole for diffusion in liquid-liquid systems, while Crank and Park (1968) find the range is from 9.2 to 42.2 Kjoule/mole for the diffusion of counter-ions in ion exchange polymers. The values found in this study, 9.2 to 48.5 Kjoule/mole, are in the same range, thus supporting the hypothesis that the process is one of diffusion.

APPLICATION

The results indicate that the time constants for ion-selective electrodes are in the range of 0.5 to 10 seconds at room temperature. For most control applications, these time constants are small enough to be ignored. However, for processes in which there is a large flow rate or a small holdup value, the process time constants are smaller. As these process time constants approach the order of magnitude of the time constants for an ion-selective electrode, the electrode time constants become more significant in the performance of the control system. It also can be concluded that a control system which operates well at one temperature may perform less well at a lower temperature where the time constants of the electrodes are greater.

CONCLUSIONS

A first-order response system is an adequate model for a glass membrane electrode. A second-order response system with effective time delay is required to model a liquid ion-exchange membrane electrode.

Theoretically it is shown that the time constants of ion-selective electrodes are inversely proportional to the diffusion coefficients.

The temperature of the fluid in which the ionic species is being measured has a strong effect on the dynamic response of the electrode, especially near the lower end of the operating temperature range.

The combination of a special low-hold-up measuring cell and pulse testing technique can be used to obtain time constant data free of any cell mixing effects.

NOTATION

A = cross-sectional area for diffusion in Equation (1), cm^2
A' = constant in Equation (22)
a_1 = constant used in Equation (17)
a_2 = constant used in Equation (21)
B = slope of linear calibration of light source and photocell system
c = concentration along the diffusion path, mole/liter
c_A = average concentration in boundary layer, mole/liter
c_1 = concentration at $x = 0$, mole/liter
c_2 = concentration at $x = L$, mole/liter
d = differential operator
D = diffusion coefficient, cm^2/s
e = base of natural logarithm, 2.7183...
f = function
F = flow rate, ml/s
$G(s)$ = transfer function
L = diffusion path length, cm
Ln = natural logarithm
log = common logarithm
m = slope defined in Equation (17), 1/°K
M.R. = magnitude ratio
n = number of the term in Equation (6)
R = gas law constant, 0.001987 Kcal/g-mole-°K
s = LaPlacian complex variable
t = time, s
T = absolute temperature, °K
V = cell volume, ml
x = distance along the diffusion path, cm
∂ = partial-differentiation operator
ΔH^* = apparent activation energy, kcal/mole

Greek Letters

τ = time constant, s
τ_D = effective time delay constant in Equation (13), s
τ_1 = first time constant in Equation (13), s
τ_2 = second time constant in Equation (13), s
ϕ = phase angle, radians
ω = angular frequency, radians/s

LITERATURE CITED

Crank, J., *The Mathematics of Diffusion*, p. 45, Oxford Univ. Press, England (1970).

———., and G. S. Park, *Diffusion in Polymers*, p. 414, Academic Press, New York (1968).

Disteche, A., and M. Dubisson, "Transient Response of the Glass Electrode to pH Step Variations," *Rev. Scientific Instruments*, **25**, 869 (1954).

Fick, A., "Ueber Diffusion," *Pogg. Ann.*, **94**, 59 (1855).

Geerings, M. W., "Dynamic Behavior of pH-Glass Electrodes and of Neutralization Process" in *Plant and Process Dynamic Characteristics*, p. 101-130, Academic Press, New York (1957).

Giusti, Jr., A. L., "The Dynamic Response of a pH Electrode in Flowing Aqueous Solutions," M.S. thesis, St. Louis Univ., Missouri (1960).

Harriott, P., *Process Control*, p. 351-2, McGraw-Hill, New York (1964).

Hays, J. R., W. C. Clements, Jr., and K. B. Schnelle, Jr., "Fortran Program for Computing Frequency Response from Pulse Test Data," Report, Vanderbilt Univ. distributed through Instrum. Soc. of America (1964).

Hougen, J. O., "Experiences and Experiments with Process Dynamics," *Chem. Eng. Monograph Ser. No. (4)*, **60**, 49 (1964).

Jost, W., *Diffusion in Solids, Liquids, Gases*, p. 293-5, Academic Press, New York (1952).

Light, T. S., "Industrial Analysis and Control With Ion-Selective Electrodes" in *Ion-Selective Electrodes*, Nat. Bur. of Standards Spec. Publ. 314, 349 (1969).

Mischke, C. R., *An Introduction to Computer-Aided Design*, p. 89-92, Prentice-Hall, Englewood Cliffs, N. J.

Murrill, P. W., *Automatic Control of Processes*, p. 193-6, Intern. Textbook, Scranton, Pa. (1967).

Ross, Jr., J. W., "Solid State and Liquid Membrane Ion-Selective Electrodes" in *Ion-Selective Electrodes*, Nat. Bur. of Standards Spec. Publ. 314, 57 (1969).

Manuscript received July 12, 1972; revision received November 17, 1972; paper accepted November 20, 1972.

Impurity Effects in Continuous-Flow Mixed Suspension Crystallizers

The crystallization of NaCl in the presence of Pb^{++} as an impurity in a continuous, mixed suspension, mixed product removal (CMSMPR) crystallizer was investigated. The results indicated that nucleation and growth rates as well as the dominant crystal sizes can be correlated by simple power functions of impurity concentration. The exponents are constants independent of the impurity concentration, thus permitting the prediction of nucleation rates, growth rates and size distributions at various concentrations of that impurity. This model was shown to apply also to other crystallizing systems.

YIH-AN LIU and GREGORY D. BOTSARIS

Department of Chemical Engineering
Tufts University
Medford, Massachusetts 02155

SCOPE

Additives have been used extensively in crystallization practice. They are often added in very small concentrations in supersaturated solutions in order to retard the nucleation of new crystals, to affect the growth rate of existing crystals, to change their habit (or form), and to improve the quality of the product through the formation of well-formed crystals.

An important practical question is whether or not one can predict the effect a particular impurity would have on a given crystallizing system; or the opposite question: If a particular effect is desired which impurity should be selected? These questions are far from being answered. The selection of an impurity continues to be an art.

The next best thing, however, would be to be able to predict the effect an impurity would have when used at

* The terms additive and impurity will be used interchangeably in this paper.

Correspondence concerning this paper should be addressed to G. D. Botsaris. Y. A. Liu is with the Department of Chemical Engineering, Princeton University, Princeton, New Jersey 08540.